environments

Article

Selective Removal and Recovery of Radioactive Cesium Ions Using DNA Aptamer-Based Systems

Sun Young Lee [1,†], Dae Hyuk Jang [2,†], Kyoon-Ho Cha [3,*] and Miyong Yun [1,2,*]

[1] Faptamer Inc., Seoul 05006, Republic of Korea; sy1106@faptamer.com
[2] Laboratory of Functional Aptamer, Department of Bioindustry and Bioresource Engineering, College of Life Sciences, Sejong University, Seoul 05006, Republic of Korea; nisclist@nate.com
[3] Department of Quantum and Nuclear Engineering, Sejong University, Seoul 05006, Republic of Korea
* Correspondence: khcha@sejong.ac.kr (K.-H.C.); myyun91@sejong.ac.kr (M.Y.)
† These authors contributed equally to this work.

Abstract

In this study, we developed a deoxyribonucleic acid (DNA) aptamer-based system for the selective removal and recovery of cesium ions (Cs^+). Cs^+-binding aptamers were selected using capture-based systematic evolution of ligands by exponential enrichment (capture-SELEX). Among the selected candidates, FA-Cs11 exhibited the highest binding affinity and removal efficiency. FA-Cs11 immobilized on streptavidin-coated agarose beads achieved a maximum removal efficiency of 92.8% for 10 μM Cs^+ under the tested conditions. Sequence analysis identified a conserved motif (TATCCAGAGTGACGCAGCA) and G-rich regions in FA-Cs11, which may cotribute to structural features associated with Cs^+ recognition. Specificity studies showed preferential removal of Cs^+ by FA-Cs11 compared with the tested metal ions, including Co^{2+}, Ni^{2+}, Cu^{2+}, Fe^{2+}, Mn^{2+}, Cr^{2+}, Al^{3+}, and Eu^{3+}. Thermal denaturation enabled the quantitative recovery of Cs^+ captured by the FA-Cs11-functionalized beads under the tested conditions. Furthermore, FA-Cs11 exhibited comparable removal performance toward radioactive cesium (^{137}Cs), demonstrating that the aptamer-based system retained its Cs-removal functionality under the short-term radioactive conditions evaluated in this study. Collectively, these findings demonstrate the feasibility of an aptamer-based molecular-recognition system for selective Cs^+ separation and recovery and provide a laboratory-scale proof-of-concept for its potential application in radioactive wastewater treatment.

Keywords: aptamer; cesium; radioactive wastewater; SELEX; radionuclide removal

Check for updates

Academic Editor: Joaquim Esteves Da Silva

Received: 14 August 2026
Revised: 28 October 2026
Accepted: 28 October 2026
Published: 30 October 2026

Copyright: © 2026 by the authors. Licensee MDPI, Basel, Switzerland. This article is an open access article distributed under the terms and conditions of the Creative Commons Attribution (CC BY) license.

1. Introduction

Global efforts toward decarbonization have accelerated the transition from fossil fuels to low-carbon energy sources. Among these, nuclear power has been recognized as a high-energy-density option with relatively low greenhouse gas emissions during operation [1]. However, the nuclear fuel cycle and potential severe accidents pose significant environmental and public health risks due to the release and redistribution of radionuclides.

Radiocesium isotopes, particularly ^{137}Cs and ^{134}Cs, are of particular concern owing to their high fission yields, strong gamma emissions, and long-term persistence in contaminated environments [2,3]. These radionuclides can enter aqueous environments through nuclear facility operations, decontamination and washing processes, radioactive waste treatment, and accidental releases, resulting in the contamination of process water, groundwater, and other aquatic systems. The long half-life of ^{137}Cs (~30 y) and its existence as a

highly mobile monovalent cation (Cs^+) complicate long-term monitoring and remediation. Furthermore, alkali metal ions such as Na^+ and K^+ are naturally abundant in environmental waters and are also commonly present in nuclear and industrial process waters, often at substantially higher concentrations than Cs^+. Because these ions share the same monovalent charge state as Cs^+, they can compete for available adsorption or ion-exchange sites, thereby reducing Cs^+ separation efficiency in complex aqueous systems. In addition, partitioning between dissolved and particulate phases can further complicate cesium removal. These challenges can affect the performance of conventional technologies, including ion-exchange resins and adsorption-based materials [4,5].

A variety of materials have been investigated for radiocesium removal, including zeolites, ion-exchange resins, Prussian blue and its analogues, clay minerals, and other inorganic sorbents. Zeolites and ion-exchange materials are attractive because of their relatively high sorption capacity, operational simplicity, and established use in water treatment; however, their selectivity for Cs^+ can decrease in complex matrices containing abundant competing ions. Prussian blue-based materials exhibit high affinity and selectivity toward Cs^+, but their practical performance can depend on material formulation, stability, regeneration, and the characteristics of the treated water. Inorganic mineral sorbents are generally inexpensive and robust, although regeneration and selective recovery of Cs^+ can be challenging.

To overcome these limitations, various advanced sorbents have been developed to enhance Cs^+ selectivity and adsorption capacity. Metal hexacyanoferrates, such as Prussian blue analogues, exhibit strong Cs^+ affinity via size- and charge-selective ion-exchange mechanisms [6]. Carbon-based nanomaterials and functionalized graphene oxide have also been investigated to improve adsorption kinetics and surface interactions [7]. More recently, layered sulfide materials have demonstrated highly selective Cs^+ capture under acidic conditions [8]. Biomaterial-inspired systems, including protein-based hybrid filters, have further expanded the range of available strategies [9]. Despite these advances, the practical implementation of some advanced sorbents may be constrained by factors such as synthesis complexity, cost, and regeneration requirements.

Aptamers—single-stranded DNA or RNA molecules selected through systematic evolution of ligands by exponential enrichment (SELEX)—offer a programmable platform for highly specific molecular recognition [10,11]. Their ability to adopt defined three-dimensional structures enables selective binding to diverse targets, including metal ions. In SELEX, the initial aptamer library consists of a large synthetic pool of single-stranded nucleic acid molecules containing a randomized central region flanked by fixed primer-binding sequences. The randomized region provides extensive sequence and structural diversity, from which target-responsive sequences can be progressively enriched through repeated rounds of selection and amplification. Recent studies have demonstrated aptamer-based recognition systems for metal-ion sensing and interaction analysis [12–14]. Beyond sensing applications, aptamers have also been widely investigated in diagnostics, environmental monitoring, targeted separation, and affinity-based purification owing to their high affinity and selectivity, chemical synthesizability, ease of sequence modification, and reversible folding behavior. DNA aptamers can generally tolerate thermal conditions better than protein-based recognition elements and may recover their functional conformation after thermal denaturation and cooling, which can be advantageous for regeneration-based separation systems. However, the radiation stability and long-term thermal stability of FA-Cs11 were not directly evaluated in the present study and therefore require further investigation under conditions relevant to radioactive wastewater treatment.

Despite this progress, the application of aptamers for radiocesium capture remains largely unexplored. Achieving high selectivity for Cs^+ is inherently challenging due to its large ionic radius and weak coordination properties compared with multivalent ions.

Therefore, the development of aptamer-based systems for cesium separation requires careful sequence design and integration with robust solid supports.

In this study, we report a cesium-selective DNA aptamer-based capture system developed using a capture-SELEX strategy for selective Cs^+ removal under aqueous conditions. Unlike conventional sorbents that primarily rely on ion exchange or physicochemical adsorption, the present approach employs a sequence-defined molecular-recognition element immobilized on a solid support. We evaluated the binding characteristics, selectivity, removal and recovery performance of the selected aptamer, FA-Cs11, and further examined its applicability to radioactive cesium (^{137}Cs). The present study provides a laboratory-scale proof-of-concept for the potential use of aptamer-based molecular-recognition systems in selective radiocesium separation and recovery.

2. Materials and Methods

2.1. Materials

Cesium chloride (CsCl) was purchased from Sigma-Aldrich (St. Louis, MO, USA). Streptavidin-coated magnetic nanobeads (AccuNanoBead™, 400 nm; Cat. No. TA-1015-1) were obtained from Bioneer (Daejeon, Republic of Korea). The beads consist of a silica-based matrix containing a magnetite (Fe_3O_4) core, which provides their magnetic properties, and are functionalized with streptavidin on the surface to enable immobilization of biotinylated oligonucleotides through the biotin–streptavidin interaction. Streptavidin-coated agarose beads (Pierce™ Streptavidin Agarose, Cat. No. 20353) were obtained from Thermo Scientific (Waltham, MA, USA). The O'Range Ruler DNA ladder was purchased from Thermo Fisher Scientific (Waltham, MA, USA). Agarose was obtained from Sigma-Aldrich (St. Louis, MO, USA), and SYBR Safe DNA staining dye was obtained from Invitrogen (Thermo Fisher Scientific, Waltham, MA, USA). GoTaq DNA polymerase and dNTP mix were purchased from Promega (Madison, WI, USA). Escherichia coli HIT™-DH5α competent cells were obtained from Real Biotech Corporation (Taipei, Taiwan).

2.2. Preparation of Aptamer Library

All oligonucleotides used in this study, including the single-stranded DNA (ssDNA) library, partially complementary biotinylated capture oligonucleotide, and primers, were custom-synthesized by Bioneer (Daejeon, Republic of Korea) according to the sequences specified by the authors. The ssDNA library had the sequence 5′-ATCCAGAGTGACGCAGCA–N_{40}–TGGACACGGTGGCTTAGT-3′, and the partially complementary biotinylated capture oligonucleotide had the sequence 5′-TGCGTCACTCTGGATATA-biotin-3′.

For amplification during systematic evolution of ligands by exponential enrichment (SELEX), a forward primer (5′-ATCCAGAGTGACGCAGCA-3′) and a reverse primer (5′-ACTAAGCCACCGTGTCCA-3′) were used. A biotinylated reverse primer (5′-Biotin-ACTAAGCCACCGTGTCCA-3′) was used to facilitate the regeneration of ssDNA for subsequent selection rounds. Following PCR amplification using the biotinylated reverse primer, the resulting double-stranded DNA products were incubated with streptavidin-coated magnetic beads. After washing to remove unbound DNA, strand separation was performed by treatment with 0.15 M NaOH for 10 min at room temperature. The supernatant containing non-biotinylated ssDNA was collected following magnetic separation. The recovered ssDNA solution was neutralized, purified by ethanol precipitation, and resuspended in nuclease-free water for subsequent SELEX rounds.

2.3. SELEX Procedure for Cs^+-Binding Aptamer Selection

Cs^+-binding DNA aptamers were selected using a capture-SELEX method. Briefly, streptavidin-coated magnetic beads (100 µL) were washed three times with 200 µL of

SELEX buffer (20 mM Tris-HAc, 140 mM NaCl, 5 mM KCl, and 10 mM $MgCl_2$, pH 7.4). The single-stranded DNA (ssDNA) library (100 pmol) was mixed with biotinylated capture oligonucleotides at a molar ratio of 1:8 (library oligonucleotide:capture oligonucleotide). The mixture was denatured at 95 °C for 5 min, incubated at 45 °C for 90 s, and cooled to 4 °C for 10 min to facilitate hybridization. The resulting DNA complexes were incubated with pre-equilibrated streptavidin-coated magnetic beads for 30 min at room temperature with gentle agitation, allowing the biotinylated capture oligonucleotides to be stably immobilized on the bead surface through the high-affinity biotin–streptavidin interaction without requiring an additional chemical coupling step. After immobilization, the beads were washed four times with SELEX buffer to remove unbound DNA sequences.

To improve selectivity, a negative selection step was performed once before the first round of positive selection using a mixed solution containing five non-target metal ions: Ni^{2+}, Co^{2+}, Mn^{2+}, Fe^{2+}, and Cr^{2+} (2 mM each). The immobilized DNA library was incubated with the mixed metal-ion solution to remove DNA sequences responsive to non-target metal ions. DNA sequences released from the magnetic beads during negative selection were discarded, whereas the remaining bead-bound DNA sequences were retained. The beads were subsequently washed with SELEX buffer to remove residual metal ions and released DNA sequences.

The remaining bead-bound DNA library was then incubated with Cs^+ ions for positive selection. DNA sequences that underwent Cs^+-induced conformational changes and dissociated from the capture oligonucleotides were collected and subjected to polymerase chain reaction (PCR) amplification. An additional negative selection step using the same competing metal ions (Ni^{2+}, Co^{2+}, Mn^{2+}, Fe^{2+}, and Cr^{2+}, 2 mM each) was performed once during Round 6, prior to Cs^+ positive selection, to further improve selectivity toward Cs^+.

A total of nine selection rounds were performed, with selection stringency progressively increased primarily by reducing the Cs^+ concentration and shortening the incubation time from 2 h to 1 h after Round 3. The Cs^+ concentration was initially set at 0.2 mM for 2 h in Rounds 1–3, followed by a gradual reduction in concentration and incubation time during subsequent rounds: 0.1 mM (Round 4, 1 h), 50 μM (Round 5, 1 h), 10 μM (Rounds 6–7, 1 h), 2 μM (Round 8, 1 h), and 1 μM (Round 9, 1 h).

The recovered DNA sequences were amplified by PCR, and single-stranded DNA was regenerated for subsequent selection rounds as described in Section 2.2.

2.4. Cloning and Sequencing

The enriched aptamer pool obtained from Round 8 was amplified by PCR (30 cycles) and cloned into a pBHA T vector using a TA cloning kit (Real Biotech, Taiwan). The constructs were transformed into E. coli HIT™-DH5α competent cells according to the manufacturer's instructions. Approximately 30 individual colonies were randomly selected and sequenced (COSMO Genetech, Seoul, Republic of Korea).

2.5. Measurement of Aptamer Binding Affinity by Surface Plasmon Resonance (SPR)

A Series S Sensor Chip SA (Cytiva, Germany) was used to evaluate the binding affinities of the selected aptamers toward Cs^+. Biotinylated aptamer candidates (FA-Cs1, FA-Cs4, FA-Cs9, and FA-Cs11) were prepared at a concentration of 200 nM in HBS-EP buffer (pH 7.4; GE Healthcare, Little Chalfont, UK) and immobilized onto the streptavidin-coated sensor surface through biotin–streptavidin interactions.

CsCl solutions were prepared at concentrations of 5, 10, 20, 40, 80, 160, 320, and 640 nM in HBS-EP buffer (pH 7.4) and injected over the aptamer-immobilized sensor surface. SPR measurements were performed using a Biacore T200 instrument (GE Healthcare), and

the resulting sensorgrams were analyzed using BIAevaluation (version 4.1) software with a steady-state affinity model to determine the equilibrium dissociation constants (K_D).

2.6. Sequence Cluster Analysis

Sequence similarity among selected Cs^+-binding aptamers was analyzed using ClustalW (version 2.1) for multiple sequence alignment. The aligned sequences were further visualized and analyzed using Jalview (version 2.11.2.0), enabling assessment of sequence conservation, alignment patterns, and sequence-based relationships.

2.7. Measurement of Cesium Concentrations by Inductively Coupled Plasma Optical Emission Spectroscopy (ICP-OES)

Cesium concentrations in samples collected after Cs^+ removal and thermal recovery were quantified using inductively coupled plasma optical emission spectroscopy (ICP-OES; PlasmaQuant PQ 9000, Analytik Jena AG, Jena, Germany). Prior to analysis, the collected samples were acidified with nitric acid to a final concentration of 2% (*v*/*v*) HNO_3. Cesium was quantified at an analytical wavelength of 455.531 nm. Calibration was performed using certified cesium standard solutions at concentrations of 0, 0.05, 0.1, 0.5, 1.0, and 2.0 mg/L. No ionization buffer was used. All samples were analyzed under the same instrumental conditions used for the calibration standards. ICP-OES data were processed using ASpect PQ software (version 1.2.4.0).

2.8. Cs^+ Removal and Recovery Using the Aptamer-Functionalized Column

Biotin-labeled aptamers (FA-Cs1, FA-Cs4, FA-Cs9, and FA-Cs11) were individually immobilized onto streptavidin-coated agarose beads through the specific biotin–streptavidin interaction. Briefly, 0.8 nmol of each biotin-labeled aptamer was incubated with 400 µL of streptavidin-coated agarose beads for 30 min at 25 °C. After immobilization, the beads were washed three times with binding/washing buffer containing 5 mM Tris-HCl (pH 7.4), 0.5 mM EDTA, and 1 M NaCl to remove unbound aptamers.

The aptamer-functionalized agarose beads (400 µL bed volume; bead diameter: 45–165 µm) were packed into a 0.8 mL column to form a fixed-bed affinity matrix. A schematic representation of the column configuration is provided in Supplementary Figure S2. A control column containing streptavidin-coated agarose beads without immobilized aptamers was prepared and tested under the same conditions. For the Cs^+ removal experiment, 300 µL of a 10 µM Cs^+ solution prepared in the same binding/washing buffer was applied to each aptamer-functionalized column and allowed to interact with the packed bed for 5 min at room temperature with gentle shaking of the entire column. The treated solution (300 µL) was subsequently collected from the column outlet, and the residual Cs^+ concentration was measured by ICP-OES as described in Section 2.7.

For Cs^+ recovery, Cs^+ retained by the aptamer-functionalized beads was released by thermal denaturation at 95 °C for 5 min using 300 µL of the same binding/washing buffer without added CsCl. The recovered solution was collected, and the Cs^+ concentration was measured by ICP-OES. All removal and recovery experiments were performed in triplicate.

The Cs^+ removal efficiency was calculated using the following equation:

$$\text{Removal efficiency } (\%) = [(C_0 - C_e)/C_0] \times 100$$

where C_0 is the initial Cs^+ concentration and C_e is the residual Cs^+ concentration in the solution collected after column treatment.

The Cs^+ recovery rate was calculated using the following equation:

$$\text{Recovery rate } (\%) = [C_r/(C_0 - C_e)] \times 100$$

where C_r is the concentration of Cs^+ recovered after thermal denaturation, and $(C_0 - C_e)$ represents the concentration of Cs^+ removed from the solution during column treatment.

2.9. Measurements of ^{137}Cs

A ^{137}Cs solution was prepared by diluting a stock solution (Eckert & Ziegler, Braunschweig, Germany). The prepared ^{137}Cs solution had an activity concentration of 33,333 Bq/L (33.333 Bq/mL). A total activity of 10.0 Bq, corresponding to 300 µL of the prepared solution, was used in each experiment.

The ^{137}Cs solution was applied to the FA-Cs11 aptamer-functionalized column using the same column configuration described in Section 2.8 and incubated for 5 min at room temperature with gentle shaking of the entire column, consistent with the contact time used in the stable Cs^+ removal experiment. Following incubation, the treated solution was collected from the column outlet. The removal efficiency of ^{137}Cs was evaluated by measuring radioactivity using a high-purity germanium (HPGe) detector (Mirion Technologies (Canberra), Inc., Meriden, CT, USA). Radioactivity was measured in the initial and treated solutions under the same measurement conditions, and the ^{137}Cs removal efficiency was determined by comparing the measured activities before and after treatment. All experiments were independently performed in triplicate.

The ^{137}Cs removal efficiency was calculated using the following equation:

$$^{137}\text{Cs removal efficiency } (\%) = [(A_0 - A_t)/A_0] \times 100$$

where A_0 is the initial ^{137}Cs activity before treatment and A_t is the residual ^{137}Cs activity in the solution collected after column treatment.

2.10. Specificity Evaluation of FA-Cs11

The specificity of FA-Cs11 toward Cs^+ was evaluated in a mixed-metal-ion solution containing Cs^+ and eight competing metal ions (Co^{2+}, Ni^{2+}, Cu^{2+}, Fe^{2+}, Mn^{2+}, Cr^{2+}, Al^{3+}, and Eu^{3+}). Competing metal-ion solutions were prepared from $CoCl_2$, $NiCl_2$, $CuCl_2$, $FeCl_2$, $MnCl_2$, $CrCl_2$, $AlCl_3$, and $EuCl_3$, corresponding nominally to Co^{2+}, Ni^{2+}, Cu^{2+}, Fe^{2+}, Mn^{2+}, Cr^{2+}, Al^{3+}, and Eu^{3+}, respectively. Cs^+ and all eight competing metal ions were combined in the same solution, each at a final concentration of 10 µM, in the binding/washing buffer described in Section 2.8 (pH 7.4). The experiments were performed under ambient laboratory conditions without deliberate exclusion of O_2 or CO_2. Following incubation with the FA-Cs11-functionalized beads, the residual concentrations of Cs^+ and the competing metal ions were quantified by ICP-OES using element-specific analytical wavelengths and calibration standards, with sample preparation and instrumental procedures as described in Section 2.7.

2.11. Statistical Analysis

All statistical analyses were performed using SPSS software (IBM SPSS Statistics, version 23). Data were analyzed using one-way analysis of variance (ANOVA), followed by Tukey's post hoc test for multiple comparisons. A p-value < 0.05 was considered statistically significant.

3. Results and Discussion

3.1. Selection of Cs^+-Specific DNA Aptamers by SELEX

In this study, cesium-specific DNA aptamers were selected using a capture-SELEX strategy based on a target-induced structure-switching mechanism [10,11] (Figure 1). Unlike conventional SELEX approaches that rely on immobilized target molecules, the selection cycle was initiated by preparing a random ssDNA library (Step ①), which was

annealed with biotinylated capture oligonucleotides via complementary hybridization (Step ②). The resulting hybridized complexes were subsequently immobilized onto streptavidin-coated magnetic beads (Step ③).

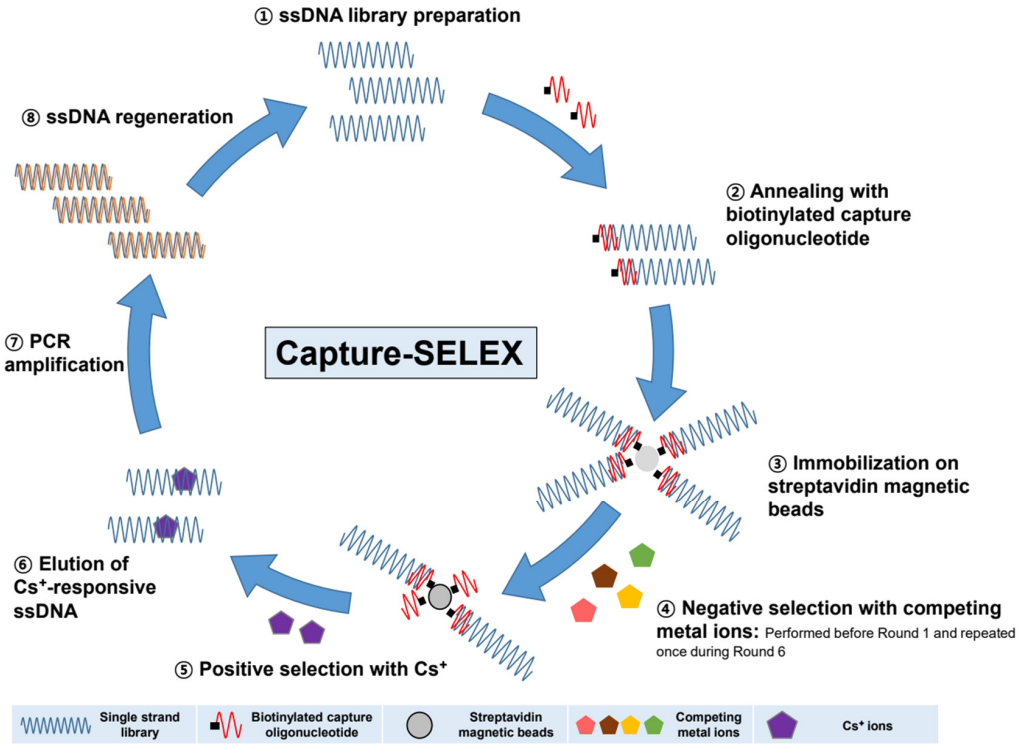


Figure 1. Schematic illustration of the capture-SELEX process for cesium-specific aptamer selection. The diagram illustrates the capture-SELEX procedure used to enrich DNA aptamers with affinity and selectivity toward Cs^+. The ssDNA library was annealed with biotinylated capture oligonucleotides and immobilized on streptavidin-coated magnetic beads. Negative selection with competing metal ions was performed before the first positive selection and repeated once during Round 6. Cs^+-responsive sequences were eluted following exposure to Cs^+, amplified by PCR, regenerated as ssDNA, and subjected to subsequent selection rounds to enrich Cs^+-binding aptamer sequences.

To improve selectivity, a negative selection step was incorporated to remove sequences showing non-specific binding to competing metal ions. This negative selection was performed once before the first round of positive selection (Step ④) and was repeated once during Round 6 using the same competing metal ions. Following negative selection, the bead-bound complexes were incubated with target Cs^+ ions for positive selection (Step ⑤). Upon exposure to Cs^+, putative Cs^+-binding sequences were expected to undergo target-induced conformational changes, facilitating their displacement and elution from the bead-bound capture strands (Step ⑥). The eluted ssDNA was collected, amplified by PCR (Step ⑦), and regenerated as single-stranded DNA (Step ⑧) for use as the input library in the subsequent selection cycle.

The progression of selection was monitored by quantifying the concentration of eluted ssDNA across the selection rounds (Figure 2). Although the amount of eluted DNA was higher in Round 5 than in Round 8, an additional negative selection step was introduced at the beginning of Round 6 to remove sequences showing nonspecific responses to competing metal ions. Following this negative selection, the concentration of recovered ssDNA temporarily decreased, consistent with the possible depletion of nonspecific sequences. In the subsequent positive-selection rounds, the recovered ssDNA concentration increased again, suggesting continued enrichment under increased selection stringency.

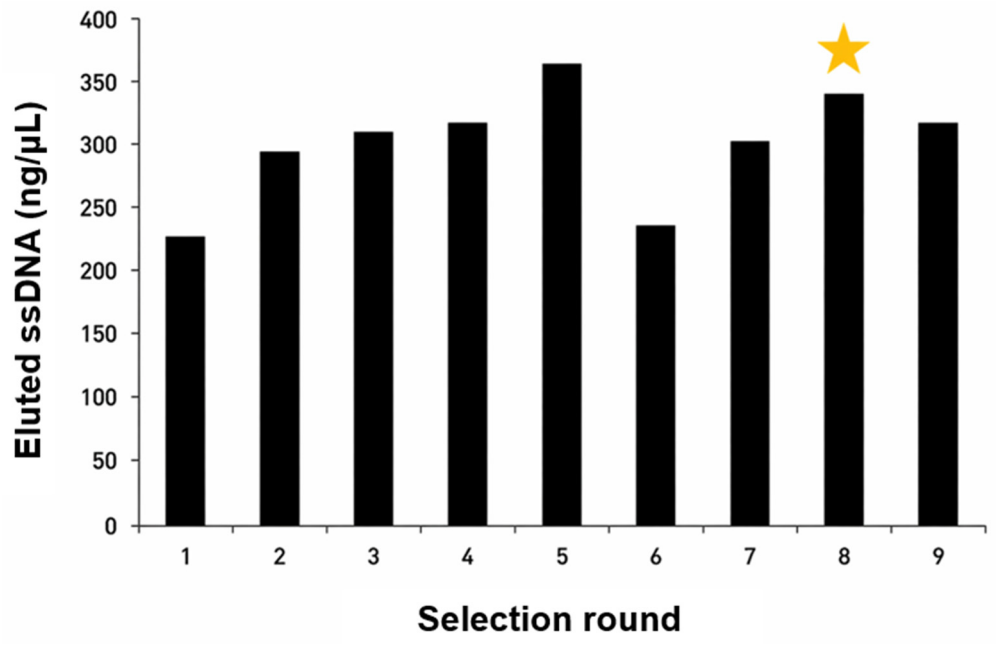


Figure 2. Screening and selection of cesium-specific DNA aptamers. The concentration of Cs^+-responsive ssDNA recovered during each selection round was monitored throughout the nine-round capture-SELEX process. Recovered DNA was amplified by PCR using a biotinylated reverse primer, and ssDNA was regenerated by alkaline strand separation using streptavidin-coated magnetic beads for subsequent selection rounds. Although a higher amount of eluted DNA was observed in Round 5, an additional negative selection step was introduced at the beginning of Round 6 to remove nonspecific sequences. The yellow star indicates Round 8, which was selected for cloning and sequencing following additional negative selection and subsequent enrichment under increased selection stringency.

Although nine selection rounds were completed, Round 8 was selected for cloning and sequencing because it represented a subsequently enriched DNA pool obtained after the additional negative selection and further positive-selection rounds, rather than because it exhibited the highest absolute amount of eluted DNA. The Round 8 pool was therefore used to identify candidate Cs^+-binding aptamer sequences for further characterization.

3.2. Binding Affinity and Structural Characterization of Cs^+-Binding Aptamers

The binding affinities of the selected aptamer candidates (FA-Cs1, FA-Cs4, FA-Cs9, and FA-Cs11) toward cesium ions (Cs^+) were evaluated using surface plasmon resonance (SPR). Biotinylated aptamers were immobilized onto a streptavidin-coated sensor surface, and CsCl solutions were injected to assess their binding responses (Figure 3A). The resulting SPR sensorgrams were analyzed using a steady-state affinity model to estimate the equilibrium dissociation constants (K_D). Among the tested candidates, FA-Cs11 exhibited the lowest estimated K_D, although the observed variability should be considered when comparing binding affinities. A summary of the aptamer sequences and their corresponding characteristics is provided in Table 1.

To further investigate the potential structural features associated with Cs^+ recognition, secondary structure prediction was performed using the mfold program based on Zuker's algorithm [15]. The predicted secondary structures of the four selected aptamers are shown in Figure 3B. These computational analyses suggested that the aptamers may form secondary structures predominantly characterized by stem–loop (hairpin) conformations.

Table 1. Sequences and characteristics of selected Cs^+-binding aptamers. Aptamers selected from the Round 8 SELEX pool were cloned and sequenced. The equilibrium dissociation constant (K_D) was estimated from surface plasmon resonance (SPR) measurements using biotinylated aptamers immobilized on a streptavidin-coated sensor surface. Lower K_D values indicate higher estimated binding affinities toward Cs^+, although experimental variability should be considered when comparing the aptamers. K_D should not be confused with the distribution coefficient (K_d) commonly used in sorption studies. The folding free energy (ΔG) of each predicted aptamer secondary structure was independently obtained using the mfold secondary-structure prediction program and was not calculated from the experimentally determined K_D values. More negative ΔG values indicate greater predicted thermodynamic stability of the folded secondary structures under the specified computational conditions. ΔG values are reported in kJ mol^{-1}. Aptamers are listed by identifier.

Aptamer	Sequence	K_D (nM)	Predicted Secondary-Structure ΔG (kJ mol^{-1})
FA-Cs1	ATCCAGAGTGACGCAGCATGCCCTAGTTAC-TACTACTCTTTTTAGCAAACGCC-CTCGCTTTGGACACGGTGGCTTAGT	50 ± 27	−35.2
FA-Cs4	ATCCAGAGTGACGCAGCATGAACGGAG-GACTCGGTGGTGCATATCCAGAGT-GACGCAGCATGGACACGGTGGCTTAGT	57 ± 21	−42.4
FA-Cs9	ATCCAGAGTGACGCAGCAGGGGGTGACGGT-GCTTGTTTATCCAGAGTGACGCAGCATGGA-CACGGTGGCTTAGT	51 ± 33	−28.5
FA-Cs11	ATCCAGAGTGACGCAGCACGACAATTCA-GAGGGAGGCTAGTATCCAGAGT-GACGCAGCATGGACACGGTGGCTTAGT	31 ± 23	−32.6

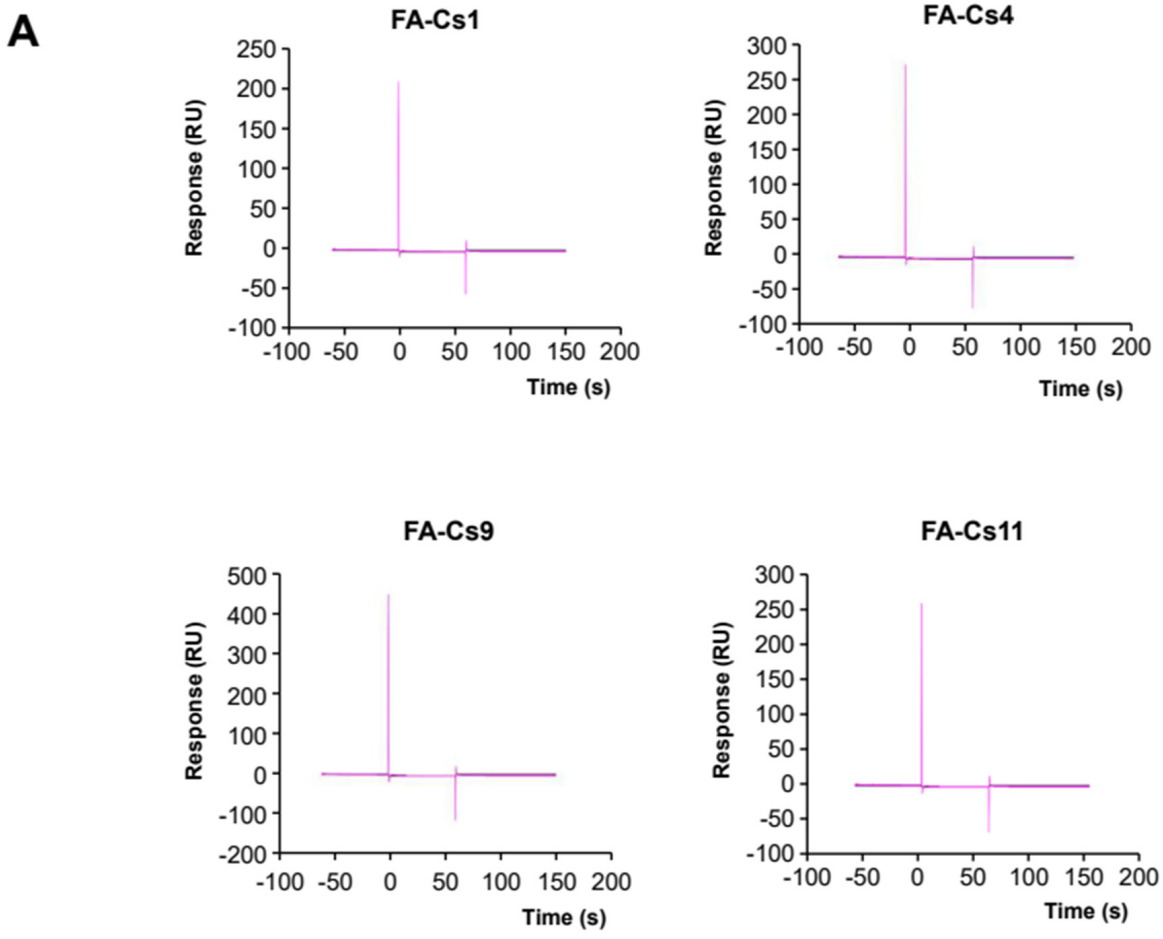


Figure 3. *Cont.*

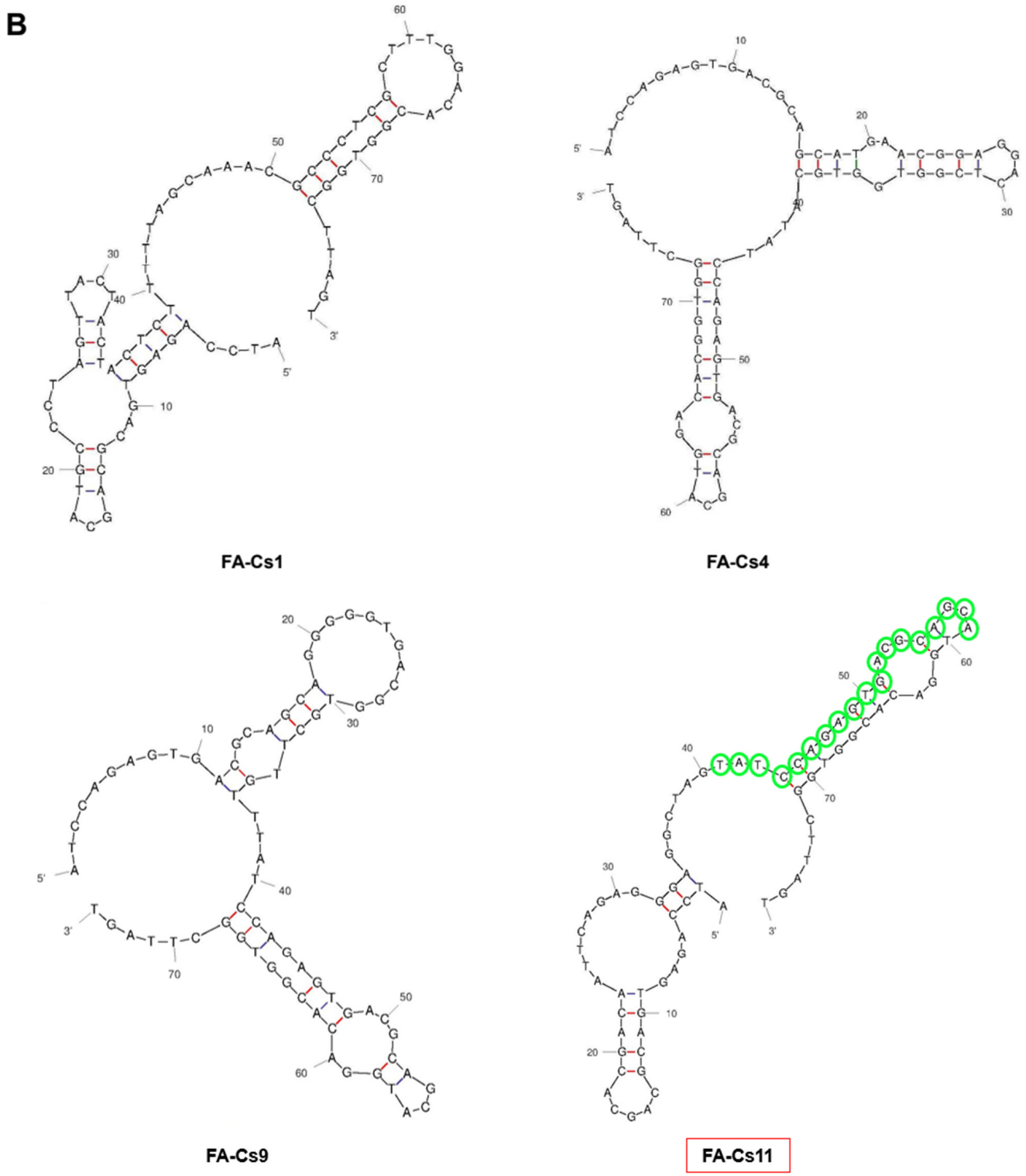


Figure 3. SPR binding analysis and predicted secondary structures of Cs^+-binding aptamers. (**A**) Surface plasmon resonance (SPR) sensorgrams showing the binding responses of Cs^+ to biotinylated aptamers (FA-Cs1, FA-Cs4, FA-Cs9, and FA-Cs11) immobilized on a streptavidin-coated sensor surface. The sensorgrams were used to estimate the equilibrium dissociation constants (K_D). The *x*-axis represents time (s), and the *y*-axis represents response units (RU). (**B**) Predicted secondary structures of the four selected Cs^+-binding aptamers, generated using Zuker's algorithm. The highlighted sequence region in FA-Cs11 represents a predicted structural feature, although its direct involvement in Cs^+ binding has not been experimentally established.

Based on the predicted structural models, Cs^+ recognition may involve structural features associated with the predicted stem–loop regions, including the highlighted sequence region in FA-Cs11, although its functional involvement in Cs^+ binding has not been experimentally established. These structural elements may contribute to the formation of a local environment favorable for Cs^+ interactions. However, the specific nucleotides involved in Cs^+ recognition, the coordination environment, and the molecular interactions responsible for binding have not been experimentally determined.

Collectively, the SPR measurements and predicted secondary structures provide preliminary insights into the potential relationship between aptamer sequence, structural organization, and Cs^+ recognition. Nevertheless, the proposed structural contributions remain hypothetical and require further experimental validation. Additional structural and mechanistic studies will be necessary to elucidate the molecular basis of Cs^+–aptamer interactions and to support the future optimization of Cs^+-binding aptamers.

3.3. Sequence Motif and Structural Analysis of Cs^+-Binding Aptamers

Sequence analysis was performed to identify conserved motifs and structural features among the selected Cs^+-binding aptamers. Multiple sequence alignments revealed a conserved sequence motif, TATCCAGAGTGACGCAGCA, within the variable regions of three of the four selected aptamers (FA-Cs11, FA-Cs4, and FA-Cs9) (Figure 4A). Several aptamers also contained guanine-rich regions, which may favor the formation of G-rich secondary structures. G-rich domains have previously been associated with cation-dependent structural organization and metal-ion recognition [16–18].

Despite these conserved features, sequence variations, including base substitutions and insertions/deletions, were observed across the aptamer pool. Phylogenetic analysis further demonstrated sequence relationships among the selected aptamers (Figure 4B), with FA-Cs4 and FA-Cs9 showing relatively high sequence similarity, whereas FA-Cs1 was more distantly related. These observations indicate that the selected aptamers retain both conserved and variable sequence features and suggest that Cs^+ recognition may not be restricted to a single sequence configuration.

Analysis of nucleotide composition showed that the guanine content of the selected aptamers ranged from approximately 29% to 33%. Predicted secondary structures also indicated the presence of hairpin-like conformations. The possible involvement of G-quadruplex-like structures remains hypothetical and requires direct structural validation.

The conserved motif and G-rich region identified in FA-Cs11 may contribute to the formation of a local structural environment involved in Cs^+ recognition. A proposed structural model is therefore presented in Supplementary Figure S1 to illustrate this hypothetical recognition environment. However, the specific binding site and molecular interactions have not been experimentally determined.

The precise hydration state and coordination environment of Cs^+ upon interaction with FA-Cs11 also remain unresolved. The present study does not distinguish between inner-sphere binding involving partial or complete dehydration of Cs^+ and outer-sphere interaction in which the hydration shell is largely retained. Therefore, the hydration state and binding mode of Cs^+ cannot be assigned from the present data. Further structural and spectroscopic studies will be required to determine the local coordination geometry, hydration state, and molecular basis of Cs^+ recognition by FA-Cs11.

In the removal process, Cs^+-containing solution is brought into contact with FA-Cs11 immobilized on streptavidin-coated agarose beads. Cs^+ is retained through interaction with the immobilized aptamer, thereby decreasing its concentration in the aqueous phase. Subsequent thermal denaturation may disrupt the aptamer conformation and

weaken its interaction with retained Cs^+, facilitating its release and recovery from the aptamer–bead matrix.

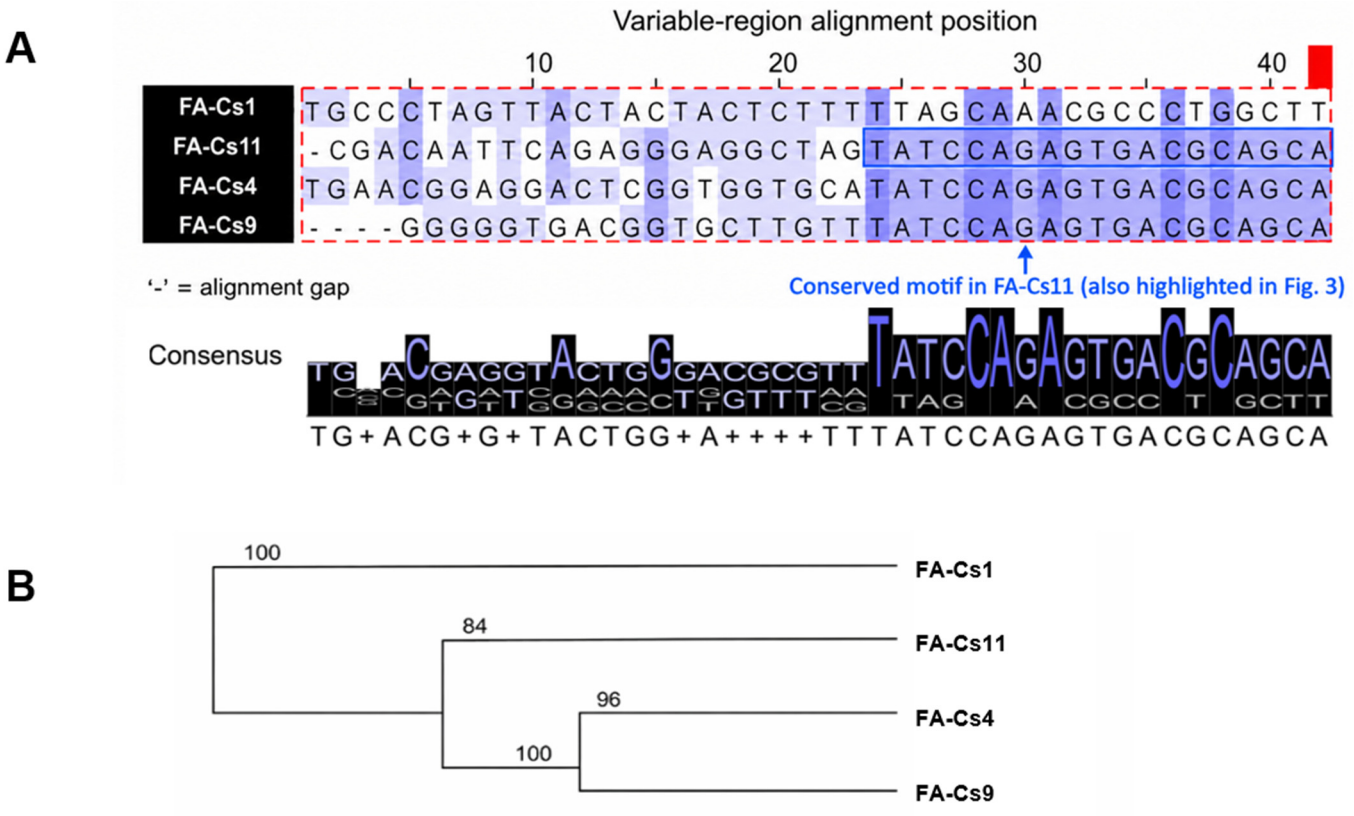


Figure 4. Sequence homology analysis of Cs^+-binding aptamers. (**A**) Multiple sequence alignment of the variable regions of the selected Cs^+-binding aptamers. The common 18-nt fixed regions at the 5′ and 3′ ends were excluded from the alignment. The numbering above the alignment indicates variable-region alignment positions, and hyphens (-) denote alignment gaps. Blue shading indicates the degree of nucleotide conservation among the aligned sequences. The conserved motif in FA-Cs11 is highlighted to facilitate comparison with the corresponding motif shown in Figure 3. (**B**) Phylogenetic tree of the selected aptamers based on sequence similarity. Numbers at the nodes indicate bootstrap support values (%).

3.4. Removal and Recovery of Cesium Ions from Aqueous Solutions Using Cs^+-Binding Aptamers

The binding affinities of the selected aptamers (FA-Cs1, FA-Cs4, FA-Cs9, and FA-Cs11) toward cesium ions (Cs^+) were evaluated as described above (Figure 3 and Table 1). To further assess their applicability for Cs^+ separation, removal and recovery experiments were performed using a column-based system.

For column preparation, biotin-labeled aptamers were immobilized onto streptavidin-coated agarose beads through the biotin–streptavidin interaction, and the aptamer-functionalized beads were packed into a column to form a fixed-bed affinity matrix. A schematic representation of the column configuration and Cs^+ removal process is provided in Supplementary Figure S2. During treatment, Cs^+-containing solution was introduced into the column, where Cs^+ interacted with the immobilized aptamers and was retained within the packed bed, while the treated solution was collected from the column outlet.

Removal experiments were performed using 300 µL of 10 µM Cs^+ solution with a 5 min contact time at room temperature, as described in Section 2.8. As shown in Figure 5A, removal efficiencies differed among the selected aptamers, with FA-Cs11 exhibiting the highest removal efficiency of approximately 92.8% under the tested conditions.

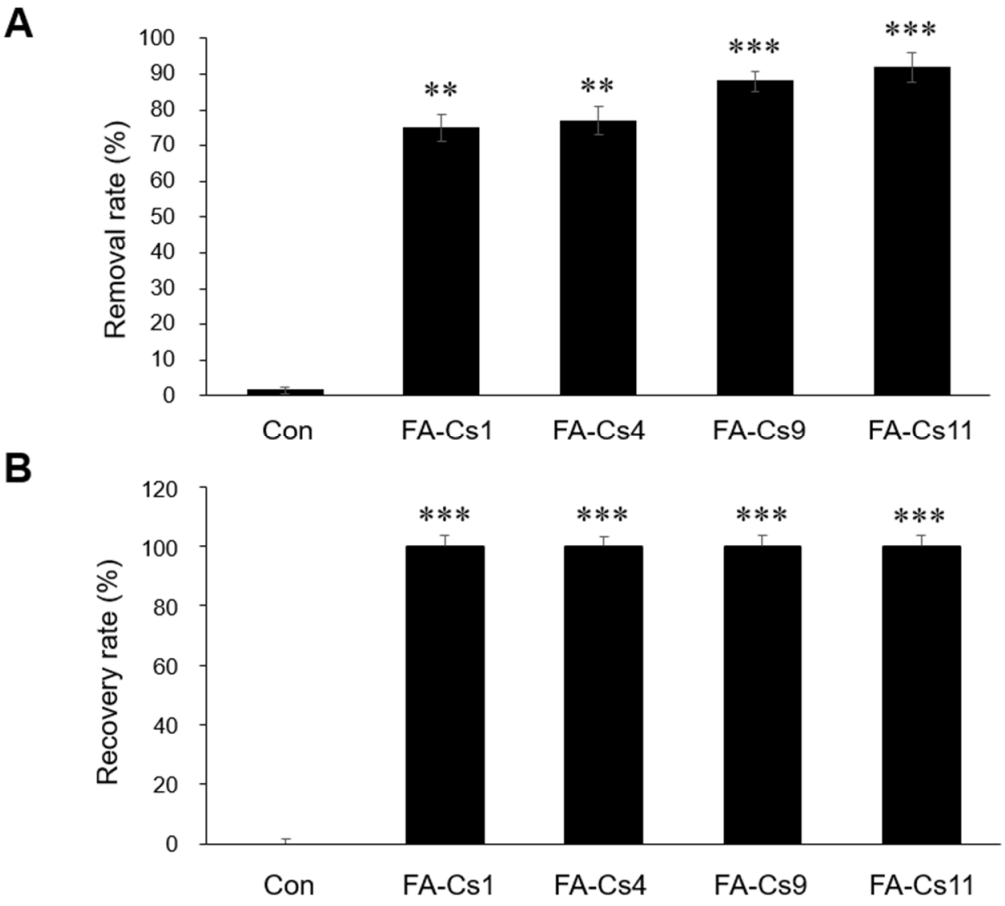


Figure 5. Removal and recovery of cesium using an aptamer–bead column. (**A**) Cs^+ removal efficiency of FA-Cs1, FA-Cs4, FA-Cs9, and FA-Cs11 under the tested column conditions (10 μM Cs^+, 300 μL, 5 min). Cs^+ concentrations before and after column treatment were measured by ICP-OES. (**B**) Cs^+ recovery rate from the aptamer–bead column. Cs^+ retained by the aptamer-functionalized beads was released by thermal denaturation at 95 °C for 5 min and quantified by ICP-OES. All experiments were performed in triplicate. Con: control column containing streptavidin-coated agarose beads without immobilized aptamers. Error bars represent standard deviation ($n = 3$). ** $p < 0.01$ and *** $p < 0.001$ versus control.

The recovery of Cs^+ retained by the aptamer–bead complex was subsequently evaluated by thermal denaturation. As shown in Figure 5B, the tested aptamers exhibited high recovery efficiencies, approaching 100% under the experimental conditions. In particular, the near-complete recovery of Cs^+ from the FA-Cs11-based system indicates that captured Cs^+ can be efficiently released from the immobilized aptamer. Previous studies have reported that aptamer-based systems can retain binding functionality over repeated regeneration cycles [19,20]. These findings suggest that the FA-Cs11-based column may have regeneration potential; however, repeated-use performance, long-term cycling stability, and operational lifetime were not evaluated in the present study. Once the aptamer-functionalized material reaches the end of its usable lifetime, any spent material retaining residual radiocesium would need to be managed as secondary radioactive solid waste in accordance with applicable radioactive-waste management requirements. The final conditioning and disposal of the spent material were not evaluated in this study.

Conventional sorbents used for Cs^+ removal include zeolites, ion-exchange resins, Prussian blue and its analogues, clay minerals, ammonium phosphomolybdate-based materials, and other inorganic ion exchangers [21–23]. Depending on the material, these sorbents may provide advantages such as relatively high sorption capacity, operational simplicity,

chemical robustness, or relatively low cost. Their performance, however, can be influenced by water composition, ionic strength, competing ions, and regeneration conditions. In practical radioactive wastewater, Cs^+ may also coexist with other radionuclides such as ^{90}Sr, and broad-spectrum sorbents may therefore provide advantages when simultaneous removal of multiple radionuclides is required. In contrast, the potential role of the FA-Cs11-based system is as a Cs-selective molecular-recognition and recovery material, rather than as a universal replacement for conventional sorbents. The present results do not establish superiority of the FA-Cs11 system over conventional sorbents in terms of sorption capacity, treatment throughput, durability, or cost.

The present FA-Cs11-based system has only been demonstrated at the laboratory scale. Practical application to large-volume radioactive wastewater treatment would require further evaluation of key process parameters, including ligand loading, column throughput, mass-transfer and hydraulic behavior, breakthrough performance, regeneration lifetime, and aptamer synthesis and immobilization costs. Because these process-scale parameters were not investigated, neither industrial-scale feasibility nor a quantitative cost advantage over established cesium sorbents can currently be established.

A further limitation is that CsCl was used as the sole Cs^+ source in the stable cesium removal and recovery experiments, and the performance of FA-Cs11 was not evaluated using other cesium salts or complex wastewater matrices. Because counter-anions, ionic strength, pH, and coexisting ions may influence aptamer folding and binding behavior, further studies using different cesium compounds and simulated or actual radioactive wastewater will be required to determine the robustness and practical applicability of the FA-Cs11-based system under realistic conditions.

Overall, these results demonstrate the effective removal and recovery of Cs^+ by the FA-Cs11-functionalized column under the tested laboratory-scale conditions and support its potential as a sequence-defined, Cs-selective affinity material. However, the present study should be regarded as a laboratory-scale proof-of-concept rather than as a demonstration of an industrial-scale treatment technology.

3.5. Removal of Radioactive Cesium (^{137}Cs) Using the Cs^+-Binding Aptamer FA-Cs11

Based on the superior removal performance observed among the selected aptamers, FA-Cs11 was further evaluated for its ability to remove radioactive cesium (^{137}Cs). The removal efficiency of ^{137}Cs was assessed using the same column configuration, treatment volume, and contact time as those used for stable Cs^+, but at the specified radioactive activity level.

As shown in Figure 6, the aptamer–bead system exhibited efficient removal of ^{137}Cs, with removal performance comparable to that observed for stable Cs^+ under the tested conditions. These results demonstrate the removal of ^{137}Cs by the FA-Cs11-based system during the short-term experiment. However, the present study did not directly evaluate radiation-induced structural damage or long-term radiation stability of the aptamer.

Because of the long half-life of ^{137}Cs relative to the 5 min treatment period, radioactive decay during the experiment was negligible and could not account for the observed decrease in ^{137}Cs activity.

Conventional Cs^+ sorbents may exhibit reduced performance in complex aqueous matrices depending on ionic strength, competing ions, and other solution conditions [24,25]. In comparison, the FA-Cs11-based system provides a sequence-defined molecular-recognition approach that may offer advantages for selective Cs^+ separation. However, direct superiority over conventional adsorbents in terms of sorption capacity, treatment throughput, durability, or cost was not established in the present study.

When considered together with the high Cs^+ recovery observed following thermal denaturation (Figure 5B), these results support the feasibility of the FA-Cs11 aptamer–bead system as a laboratory-scale platform for radioactive cesium separation, with potential for subsequent recovery based on the stable Cs^+ experiments. Further studies are required to evaluate long-term regeneration performance, radiation stability, treatment capacity, and performance in complex radioactive wastewater matrices before practical or large-scale application can be established.

Collectively, these findings demonstrate that the FA-Cs11 aptamer-based system can remove radioactive cesium under the tested laboratory conditions and support its further investigation as a selective Cs^+ separation material.

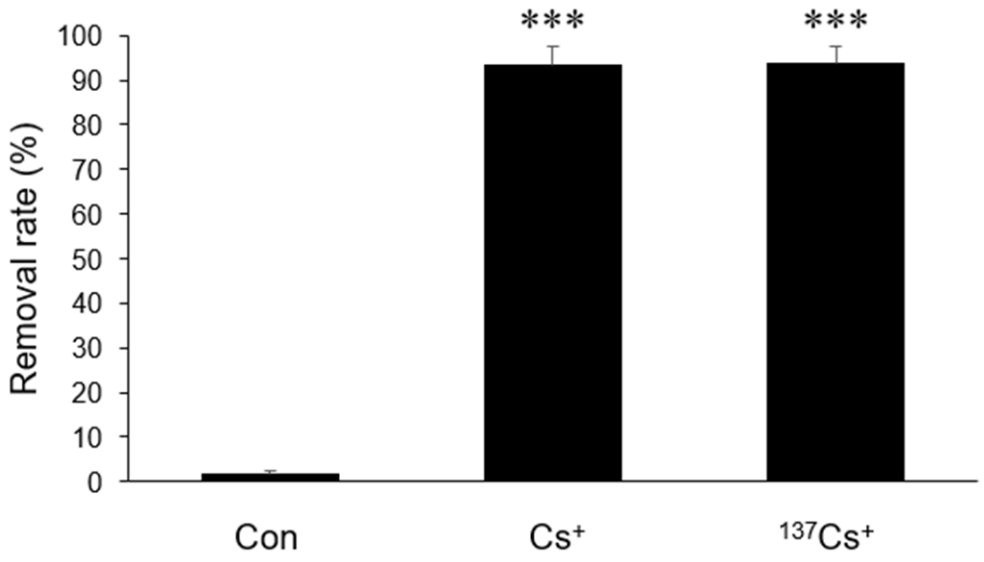


Figure 6. Comparison of removal efficiency between stable cesium (Cs^+) and radioactive cesium (^{137}Cs) using the FA-Cs11 aptamer–bead system. For stable Cs^+, cesium concentrations before and after treatment with the FA-Cs11 aptamer-functionalized column were measured by ICP-OES. For ^{137}Cs, radioactivity before and after treatment with the FA-Cs11 aptamer-functionalized column was measured using an HPGe detector. All experiments were independently performed in triplicate. Con: control column containing streptavidin-coated agarose beads without immobilized aptamers. Error bars represent standard deviation ($n = 3$). *** $p < 0.001$ versus control.

3.6. Specificity of Cs^+-Binding Aptamer FA-Cs11

To further evaluate the binding specificity of the selected aptamer, FA-Cs11, competitive binding experiments were conducted in the presence of Cs^+ and eight competing metal ions (Co^{2+}, Ni^{2+}, Cu^{2+}, Fe^{2+}, Mn^{2+}, Cr^{2+}, Al^{3+}, and Eu^{3+}) in the same solution. Cs^+ and each competing metal ion were tested at the same concentration of 10 μM to allow direct comparison of their interactions with FA-Cs11.

As shown in Figure 7, FA-Cs11 exhibited a Cs^+ removal efficiency of approximately 70% in the presence of multiple coexisting metal ions, whereas the removal efficiencies observed for the other metal ions were generally below 20%. These results indicate that FA-Cs11 preferentially removed Cs^+ relative to the other tested metal ions under the tested competitive conditions.

The preferential removal of Cs^+ suggests that FA-Cs11 may recognize physicochemical and structural features of Cs^+ through sequence-dependent conformational arrangements. As discussed above, the conserved motif and G-rich regions of FA-Cs11 may contribute to the formation of a local structural environment favorable for Cs^+ recognition; however, the precise molecular basis of this selectivity has not yet been experimentally established.

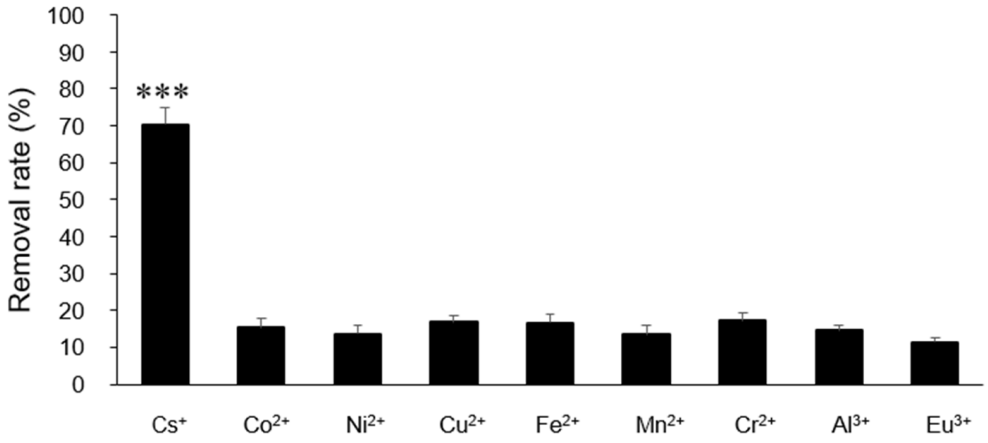


Figure 7. Specificity of the Cs^+-binding aptamer FA-Cs11. Removal efficiencies of various metal ions by the FA-Cs11 aptamer–bead column in a mixed-metal-ion solution containing Cs^+ and eight competing metal ions (Co^{2+}, Ni^{2+}, Cu^{2+}, Fe^{2+}, Mn^{2+}, Cr^{2+}, Al^{3+}, and Eu^{3+}), each at a final concentration of 10 μM. The concentrations of metal ions were measured by ICP-OES before and after incubation with the FA-Cs11-functionalized column for 5 min under gentle shaking, followed by collection of the treated solution from the column outlet. All experiments were performed in triplicate. Removal efficiency (%) was calculated as [(initial ion concentration − residual ion concentration)/initial ion concentration] × 100. Error bars represent standard deviation ($n = 3$). *** $p < 0.001$ indicates a statistically significant difference in removal efficiency between Cs^+ and each of the eight competing metal ions.

The competing metal ions were introduced using their corresponding chloride salts and are therefore referred to according to their nominal oxidation states. However, the actual aqueous speciation and oxidation states of these ions were not independently characterized during the experiments. Under the tested conditions (pH 7.4 and ambient laboratory atmosphere), redox-sensitive ions, particularly Fe and Cr, may undergo changes in oxidation state in the presence of oxygen. In addition, exposure to CO_2 may influence metal speciation through carbonate complexation or, for some metal ions, the possible formation of sparingly soluble phases. Furthermore, the binding/washing buffer contained 0.5 mM EDTA, which may form complexes with the tested metal ions and influence their apparent removal efficiencies. Accordingly, the observed removal efficiencies should be interpreted as responses under the tested experimental conditions rather than as intrinsic binding affinities toward rigorously defined individual metal species.

Another limitation of the present study is that the concentration-dependent effect of Na^+ and the competitive effect of K^+ were not independently evaluated. Although the binding/washing buffer contained 1 M NaCl, the influence of varying Na^+ concentrations on Cs^+ removal was not systematically investigated. Because Na^+, K^+, Ca^{2+}, and Mg^{2+} are commonly present in natural and process waters and may influence Cs^+ separation performance, their effects should be systematically examined at environmentally relevant concentrations. In addition, although all experiments were conducted at pH 7.4, the pH dependence of FA-Cs11 folding and Cs^+ binding was not systematically investigated. Changes in pH may affect nucleobase protonation, aptamer conformation, metal-ion speciation, and aptamer–ion interactions.

Therefore, further studies under controlled pH, redox, and CO_2 conditions, as well as systematic evaluation of the effects of Na^+, K^+, Ca^{2+}, and Mg^{2+} at environmentally relevant concentrations, will be required to more rigorously evaluate the selectivity of FA-Cs11 and its applicability in complex radioactive wastewater matrices.

4. Conclusions

This study demonstrates the feasibility of a DNA aptamer-based system for the selective recognition, removal, and recovery of Cs^+ under laboratory-scale conditions. Using a capture-SELEX strategy, several Cs^+-binding aptamer candidates were identified, among which FA-Cs11 exhibited the highest removal efficiency. The FA-Cs11 aptamer-functionalized system achieved a maximum Cs^+ removal efficiency of 92.8% under the tested conditions. Specificity experiments further showed that FA-Cs11 exhibited preferential removal of Cs^+ in a mixed-metal-ion solution containing Co^{2+}, Ni^{2+}, Cu^{2+}, Fe^{2+}, Mn^{2+}, Cr^{2+}, Al^{3+}, and Eu^{3+}.

Sequence and predicted secondary-structure analyses identified a conserved motif (TATCCAGAGTGACGCAGCA), G-rich regions, and hairpin-like structural features in the selected aptamers. These sequence characteristics and predicted secondary structures provide a basis for investigating the molecular determinants of Cs^+ recognition. The conserved motif and G-rich regions could contribute to Cs^+ recognition through sequence-dependent structural organization; however, the involvement of specific structures, including possible G-quadruplex-like conformations, remains a hypothesis requiring direct structural and mechanistic validation.

Thermal denaturation enabled the release and recovery of Cs^+ captured by the FA-Cs11-functionalized material, with recovery rates approaching 100% under the tested conditions. This result indicates the potential for regeneration of the aptamer-functionalized material; however, long-term regeneration performance, repeated-cycle stability, and operational lifetime were not evaluated in the present study. Conventional ion-exchange resins and related sorbent materials remain established approaches for radionuclide removal and may be regenerated and reused depending on the material and operating conditions [4,26]. Accordingly, the present results should not be interpreted as demonstrating reduced secondary-waste generation.

The FA-Cs11-based system also removed ^{137}Cs under the short-term radioactive conditions examined, with removal performance comparable to that observed for stable Cs^+. These results demonstrate its short-term ^{137}Cs removal capability, but do not establish long-term radiation stability of the aptamer or column material. Previous studies have also reported the application of DNA aptamers to other metal ions, including cobalt and nickel [27,28], supporting the broader potential of aptamer-based molecular-recognition approaches for selective metal-ion separation.

Overall, the present study provides a laboratory-scale proof-of-concept for the use of FA-Cs11 as a sequence-defined recognition element for selective Cs^+ separation and recovery. The present results do not establish superiority over conventional sorbents in terms of sorption capacity, treatment throughput, durability, cost, or waste generation. Further studies should evaluate the molecular basis of Cs^+ recognition, long-term regeneration and radiation stability, column breakthrough and treatment capacity, and performance in complex radioactive wastewater matrices before practical or large-scale application can be established.

Supplementary Materials: The following supporting information can be downloaded at: https://www.mdpi.com/article/10.3390/environments13110596/s1. Figure S1: Proposed schematic structural model of FA-Cs11 for Cs^+ recognition; Figure S2: Schematic illustration of the FA-Cs11 aptamer-functionalized packed-bed column for Cs^+ removal.

Author Contributions: Conceptualization, S.Y.L. and D.H.J.; methodology, S.Y.L. and D.H.J.; software, S.Y.L. and D.H.J.; validation, S.Y.L. and D.H.J.; formal analysis, S.Y.L. and D.H.J.; investigation, S.Y.L. and D.H.J.; resources, K.-H.C. and M.Y.; data curation, S.Y.L. and D.H.J.; writing—original draft preparation, S.Y.L. and D.H.J.; writing—review and editing, S.Y.L.; visualization, S.Y.L. and D.H.J.;

supervision, M.Y.; project administration, K.-H.C. and M.Y.; funding acquisition, K.-H.C. and M.Y. All authors have read and agreed to the published version of the manuscript.

Funding: This work was supported by the Commercialization Promotion Agency for R&D Outcomes (COMPA), funded by the Ministry of Science and ICT (MSIT) [No. RS-2025-02634691], and by the National Research Foundation of Korea (NRF), funded by the Korean government (MSIT) [Nos. 2023R1A2C1006127 and RS-2025-02353161].

Data Availability Statement: The data presented in this study are available from the corresponding authors upon reasonable request.

Conflicts of Interest: Miyong Yun is the Chief Executive Officer and a shareholder of Faptamer Inc. Sun Young Lee is an employee and a shareholder of Faptamer Inc. Dae Hyuk Jang and Kyoon-Ho Cha are shareholders of Faptamer Inc. but are not employees of the company. Faptamer Inc. is engaged in the research and development of aptamer-based technologies. The authors declare no other conflicts of interest.

Abbreviations

The following abbreviations are used in this manuscript: DNA, deoxyribonucleic acid; ssDNA, single-stranded DNA; SELEX, systematic evolution of ligands by exponential enrichment; SPR, surface plasmon resonance; ICP-OES, inductively coupled plasma optical emission spectroscopy; HPGe, high-purity germanium; PCR, polymerase chain reaction; K_D, equilibrium dissociation constant; RU, response units.

References

1. Rogner, H.-H. Energy resources and potentials. In *Global Energy Assessment (GEA)*; Johansson, T.B., Patwardhan, A., Nakicenovic, N., Echeverri, L.G., Eds.; Cambridge University Press: New York, NY, USA, 2012; pp. 425–512.
2. United Nations Scientific Committee on the Effects of Atomic Radiation (UNSCEAR). *Sources, Effects and Risks of Ionizing Radiation, UNSCEAR 2013 Report*; United Nations: New York, NY, USA, 2013; Volume I, pp. 25–116.
3. Steinhauser, G.; Brandl, A.; Johnson, T.E. Comparison of the Chernobyl and Fukushima nuclear accidents: A review of the environmental impacts. *Sci. Total Environ.* **2014**, *470–471*, 800–817, Erratum in *Sci. Total Environ.* **2014**, *487*, 575. [CrossRef] [PubMed]
4. Sylvester, P. Developments in ion exchange and adsorption processes for radioactive waste treatment. In *Advanced Separation Techniques for Nuclear Fuel Reprocessing and Radioactive Waste Treatment*; Nash, K.L., Lumetta, G.J., Eds.; Woodhead Publishing: Cambridge, UK, 2010; pp. 377–411.
5. Sayed, M.A.; Helal, A.I.; Abdelwahab, S.M.; Aly, H.F. Sorption of cesium from aqueous solutions by some Egyptian pottery materials. *Appl. Clay Sci.* **2017**, *139*, 1–8. [CrossRef]
6. Feng, S.; Ni, J.; Cao, X.; Gao, J.; Yang, L.; Jia, W.; Chen, F.; Feng, S.; Zhang, Y.; Ma, F. Separation and Removal of Radionuclide Cesium from Water by Biodegradable Magnetic Prussian Blue Nanospheres. *Processes* **2022**, *10*, 2492. [CrossRef]
7. Sabzehmeidani, M.M.; Mahnaee, S.; Ghaedi, M.; Heidari, H.; Roy, V.A.L. Carbon based materials: A review of adsorbents for inorganic and organic compounds. *Mater. Adv.* **2021**, *2*, 598–627. [CrossRef]
8. Tang, J.-H.; Jin, J.-C.; Li, W.-A.; Zeng, X.; Ma, W.; Li, J.-L.; Lv, T.-T.; Peng, Y.-C.; Feng, M.-L.; Huang, X.-Y. Highly selective cesium(I) capture under acidic conditions by a layered sulfide. *Nat. Commun.* **2022**, *13*, 658. [CrossRef] [PubMed]
9. Chiera, N.M.; Bolisetty, S.; Eichler, R.; Mezzenga, R.; Steinegger, P. Removal of radioactive cesium from contaminated water by whey protein amyloids–carbon hybrid filters. *RSC Adv.* **2021**, *11*, 32454–32458. [CrossRef] [PubMed]
10. Tuerk, C.; Gold, L. Systematic evolution of ligands by exponential enrichment: RNA ligands to bacteriophage T4 DNA polymerase. *Science* **1990**, *249*, 505–510. [CrossRef] [PubMed]
11. Ellington, A.D.; Szostak, J.W. In vitro selection of RNA molecules that bind specific ligands. *Nature* **1990**, *346*, 818–822. [CrossRef] [PubMed]
12. Yoshida, K.; Hayashi, T.; Takinoue, M.; Onoe, H. Repeatable detection of Ag+ ions using a DNA aptamer-linked hydrogel biochemical sensor integrated with microfluidic heating system. *Sci. Rep.* **2022**, *12*, 9692. [CrossRef] [PubMed]
13. Zhu, J.; Wang, D.; Yu, H.; Yin, H.; Wang, L.; Shen, G.; Geng, X.; Yang, L.; Fei, Y.; Deng, Y. Advances in colorimetric aptasensors for heavy metal ion detection utilizing nanomaterials: A comprehensive review. *Anal. Methods* **2023**, *15*, 6320–6343. [CrossRef] [PubMed]
14. Bao, W.; Aodeng, G.; Ga, L.; Ai, J. Aptamer-based electrochemical biosensors: Signal transduction mechanisms, application progress, and future trends. *Sens. Actuators Rep.* **2025**, *10*, 100366. [CrossRef]

15. Zuker, M. Mfold web server for nucleic acid folding and hybridization prediction. *Nucleic Acids Res.* **2003**, *31*, 3406–3415. [CrossRef] [PubMed]
16. Liu, Y.; Wang, X.; Liu, J. Unexpected enrichment of DNA aptamers for Zn^{2+} ions from an insulin selection. *Chem. Commun.* **2024**, *60*, 6280–6283. [CrossRef] [PubMed]
17. Xia, T.; Yuan, J.; Fang, X. Conformational Dynamics of an ATP-Binding DNA Aptamer: A Single-Molecule Study. *J. Phys. Chem. B* **2013**, *117*, 14994–15003. [CrossRef] [PubMed]
18. Jang, D.; Lee, S.Y.; Kim, W.-S.; Rhee, K.-J.; Kim, E.-O.; Yun, M. Manganese Removal from the Seo-Gok Reservoir Water Using DNA Aptamers. *Environments* **2025**, *12*, 99. [CrossRef]
19. Potyrailo, R.A.; Murray, A.J.; Nagraj, N.; Pris, A.D.; Ashe, J.M.; Todorovic, M. Towards maintenance-free biosensors for hundreds of bind/release cycles. *Angew. Chem. Int. Ed.* **2015**, *54*, 2174–2178. [CrossRef] [PubMed]
20. Sun, N.-N.; Tinnefeld, P.; Li, G.-L.; He, Z.-K.; Xu, Q.-F. Aptamer melting biosensors for thousands of signaling and regenerating cycles. *Biosens. Bioelectron.* **2025**, *271*, 116998. [CrossRef] [PubMed]
21. Mimura, H.; Lehto, J.; Harjula, R. Ion Exchange of Cesium on Potassium Nickel Hexacyanoferrate(II)s. *J. Nucl. Sci. Technol.* **1997**, *34*, 484–489. [CrossRef]
22. Vipin, A.K.; Hu, B.; Fugetsu, B. Prussian blue caged in alginate/calcium beads as adsorbents for removal of cesium ions from contaminated water. *J. Hazard. Mater.* **2013**, *258–259*, 93–101. [CrossRef] [PubMed]
23. Zhuang, S.; Wang, J. Cesium removal from radioactive wastewater by adsorption and membrane technology. *Front. Environ. Sci. Eng.* **2024**, *18*, 38. [CrossRef]
24. Jang, S.-C.; Haldorai, Y.; Lee, G.-W.; Hwang, S.-K.; Han, Y.-K.; Roh, C.; Huh, Y.S. Porous three-dimensional graphene foam/Prussian blue composite for efficient removal of radioactive ^{137}Cs. *Sci. Rep.* **2015**, *5*, 17510. [CrossRef] [PubMed]
25. Baimenov, A.; Montagnaro, F.; Inglezakis, V.J.; Balsamo, M. Experimental and Modeling Studies of Sr^{2+} and Cs^{+} Sorption on Cryogels and Comparison to Commercial Adsorbents. *Ind. Eng. Chem. Res.* **2022**, *61*, 8204–8219. [CrossRef]
26. International Atomic Energy Agency (IAEA). *Application of Ion Exchange Processes for Treatment of Radioactive Waste and Management of Spent Ion Exchangers*; Technical Reports Series No. 408; IAEA: Vienna, Austria, 2002.
27. Jang, D.H.; Lee, S.Y.; Kim, H.; Yun, M.Y. Selection of a nickel-specific DNA aptamer and development of a protocol for radioactive nickel removal. *Ann. Nucl. Energy* **2024**, *195*, 110138. [CrossRef]
28. Lee, S.Y.; Jang, D.H.; Kim, H.; Yun, M. Removal and isolation of radioactive cobalt using DNA aptamers. *Radiochim. Acta* **2023**, *111*, 357–365. [CrossRef]

Disclaimer/Publisher's Note: The statements, opinions and data contained in all publications are solely those of the individual author(s) and contributor(s) and not of MDPI and/or the editor(s). MDPI and/or the editor(s) disclaim responsibility for any injury to people or property resulting from any ideas, methods, instructions or products referred to in the content.